A Nonlinear Model Predictive Control Strategy for Glucose Control in People with Type 1 Diabetes

Boiroux, Dimitri; Jørgensen, John Bagterp

Published in:
I F A C Workshop Series

Link to article, DOI:
10.1016/j.ifacol.2018.11.644

Publication date:
2018

Document Version
Publisher's PDF, also known as Version of record

Available online at www.sciencedirect.com

ScienceDirect

IFAC PapersOnline CONFERENCE PAPER ARCHIVE

IFAC PapersOnLine 51-27 (2018) 192–197

A Nonlinear Model Predictive Control Strategy for Glucose Control in People with Type 1 Diabetes

Dimitri Boiroux, John Bagterp Jørgensen

Department of Applied Mathematics and Computer Science, Technical University of Denmark, DK-2800 Kgs. Lyngby, Denmark.

Abstract: In this paper, we evaluate the closed-loop performance of a control algorithm for the treatment of type 1 diabetes (T1D) identified from prior continuous glucose monitor (CGM) data. The control algorithm is based on nonlinear model predictive control (NMPC). At each iteration, we solve an optimal control problem (OCP) using a sequential quadratic programming algorithm with multiple shooting and sensitivity computation. The control algorithm uses a physiological model of T1D to predict future blood glucose (BG) concentrations. The T1D physiological model takes into account the dynamics between subcutaneously administered insulin and blood glucose, the contribution of meal absorption and the lag and noise of CGM measurements. The model parameters have been identified using prior data. Numerical simulations on 10 patients show that the NMPC algorithm is safe and is able to optimize the insulin delivery in patients with T1D.

Keywords: Type 1 diabetes, diabetes technology, nonlinear model predictive control, continuous-discrete extended Kalman filter.

1. INTRODUCTION

Type 1 diabetes (T1D) is an autoimmune disease causing the destruction of the insulin-producing β-cells of the pancreas. People with T1D rely on exogenously administered insulin to regulate their blood glucose (BG) concentration. Usual insulin therapy consists of a combination of basal insulin and insulin boluses. Basal insulin compensates for endogenous glucose production from the liver, whereas boluses are administered at mealtimes to mitigate postprandial glucose excursions. Currently, the decision on the amounts of insulin to administer is made by the patient him/herself.

The artificial pancreas (AP) refers to closed-loop of BG concentration for T1D, and has the potential to partially or fully automate the insulin therapy for people with T1D. Current AP prototypes comprise a CGM, a control algorithm and an insulin pump. The CGM provides frequent interstitial glucose measurements (al least every 5 minutes, but more frequent measurements are also possible). The estimator computes the state estimates and predictions through an extended Kalman filter (EKF) and identifies the parameters of the T1D model using maximum likelihood. The detector detects faulty CGM measurements, eg. drifts, as well as meal time and size by using a specific algorithm for meal estimation (Turksoy et al. (2016); Mahmoudi et al. (2016, 2017); Samadi et al. (2018)). The MPC algorithm uses the model and states provided by the Kalman filter and meal information to predict and optimize future insulin injections. Smart bolus calculators may be used to compute prandial insulin boluses (Marchetti et al. (2008); Schmidt et al. (2012); Boiroux et al. (2015, 2017)). A continuous subcutaneous insulin infusion (CSII) pump implements the suggested basal and/or boluses using the subcutaneous (sc.) route. Fig. 1 illustrates the AP.

Model predictive control (MPC) is a model-based control technology. At each iteration, the control algorithm optimizes the predicted outcome of a given system by solving an optimal control problem (OCP). Nonlinear model predictive control (NMPC) algorithms have already shown promising closed-loop performance in the case where full state information is available (Boiroux et al. (2010a)). Nonlinear filters such as the extended and unscented Kalman filters can estimate the meal size and track the insulin sensitivity (Boiroux et al. (2015)). The NMPC-based approach has the advantage to incorporate the physiological model of the patient, the constraints on insulin injections, the insulin on board, the effects of CHO absorption, the physiological lags and delays in an intuitive, unified and straightforward manner.

In this paper, we present and evaluate the closed-loop performance of a NMPC-based control algorithm for T1D with parameters identified from prior data. The physiological T1D is formulated as a stochastic model in continuous time with discrete-time measurements. We assess the performance of our control algorithm on a virtual population of 10 patients with T1D.

This paper is structured as follows. Section 2 presents the identifiable physiological model of T1D and the identified parameters for 10 virtual patients. Section 3 presents the continuous-discrete extended Kalman filter. In Section 4, we briefly state the OCP used in our control algorithm. In Section 5, we discuss the formulation of the objective

⋆ This paper is funded by The Danish Diabetes Academy supported by the Novo Nordisk Foundation.

10.1016/j.ifacol.2018.11.644

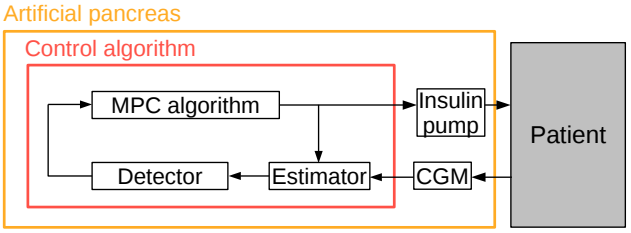

Fig. 1. Diagram of the artificial pancreas. The estimator uses an EKF to estimate states, parameters, and to compute the state predictions. The detector estimates the meals times and size and detects the CGM drifts based on the identified model and innovations provided by the estimator. The MPC algorithm optimizes the future insulin injections and computes the state predictions.

function. Section 6 illustrates the closed-loop performance of our control algorithm on a population of 10 patients. Section 7 summarizes the main contribution of this paper.

2. PHYSIOLOGICAL MODEL OF GLUCOSE-INSULIN DYNAMICS

In this section, we present a minimal physiological model derived from the model by Kanderian et al. (2009). This model describes the glucose-insulin dynamics, the meal absorption, and the lag and noise from CGMs. Fig. 2 illustrates the MVP model. The CGM noise model has been developed by Facchinetti et al. (2014). We add diffusion terms to reformulate the MVP model as a stochastic model in the form

$$dx(t) = f(t, x(t), u(t), d(t), \theta)dt + \sigma(\theta)dw(t), \quad (1a)$$
$$y_k = g(x_k) + v_k, \quad (1b)$$

in which $x(t) \in \mathbb{R}^{n_x}$ is a vector containing the states variables, and $y_k \in \mathbb{R}^{n_y}$ is a vector containing the output variables measured at discrete times. $u(t) \in \mathbb{R}^{n_u}$ is a vector containing the manipulated inputs, and $d(t) \in \mathbb{R}^{n_d}$ is a vector containing the uncontrolled disturbances. $\{w(t),\ t \geq 0\}$ is a standard Wiener process, i.e. $dw(t) \sim N(0, Idt)$. $\theta \in \mathbb{R}^{n_\theta}$ is a vector containing the parameters to be estimated. The matrix $\sigma(\theta)$ is time-invariant and assumed to be diagonal. The measurement noise, v_k, is independently normally distributed, $v_k \sim N_{iid}(0, R(\theta))$. Also, we assume that the initial state, x_0, is normally distributed with a known mean and covariance, $x_0 \sim N(\hat{x}_{0|-1}(\theta), P_{0|-1}(\theta))$.

2.1 Insulin Absorption Subsystem

The insulin absorption subsystem is given by the following two-compartment model

$$dI_{SC} = k_1 \left(\frac{u(t)}{C_I} - I_{SC}(t) \right) dt + \sigma_1 d\omega_1, \quad (2a)$$
$$dI_P = k_2 \left(I_{SC}(t) - I_P(t) \right) dt + \sigma_2 d\omega_2, \quad (2b)$$

where $I_{SC}(t)$ [mU/L/min] is the subcutaneous insulin concentration, and $I_P(t)$ [mU/L] is the plasma insulin concentration. $u(t)$ [mU/min] is the insulin infusion rate, C_I [L/min] is the clearance rate.

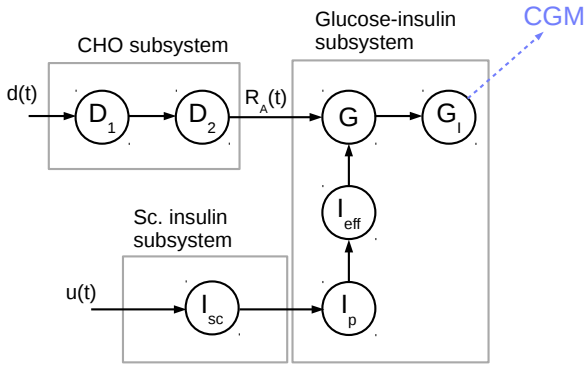

Fig. 2. The MVP model. This model simulates the action of subcutaneously administered insulin on BG concentration, the effects of meals, interstitial glucose and CGM measurements.

2.2 Insulin-Glucose Dynamics

The effect of insulin on blood glucose is described by the following SDEs

$$dI_{EFF} = \left(-p_2 I_{EFF}(t) + p_2 S_I I_P(t) \right) dt + \sigma_3 d\omega_3, \quad (2c)$$
$$dG = \left(-(I_{EFF}(t) + GEZI)G(t) + EGP + R_A(t) \right) dt + \sigma_4 d\omega_4. \quad (2d)$$

$I_{EFF}(t)$ [min^{-1}] is the effect of insulin. S_I [mL/mU] reflects the insulin sensitivity. The glucose concentration $G(t)$ [mg/dL] is also affected by the endogenous glucose production (EGP) [mg/dL/min] and the rate of appearance contribution from the meals, $R_A(t)$ [mg/dL/min].

2.3 CHO Absorption Model

We use the two-compartment model introduced by Hovorka *et al.* Hovorka et al. (2004) to describe the carbohydrates (CHO) absorption from meals and conversion to glucose. The model describes the effect of orally ingested carbohydrates on the rate of appearance of glucose $R_A(t)$ [mg/dL/min] in the blood stream. The CHO absorption model is

$$dD_1 = \left(d(t) - \frac{D_1(t)}{\tau_G} \right) dt + \sigma_5 d\omega_5, \quad (2e)$$
$$dD_2 = \left(\frac{D_1(t) - D_2(t)}{\tau_G} \right) dt + \sigma_6 d\omega_6, \quad (2f)$$
$$R_A(t) = D_2(t) \frac{k_m}{V_G}. \quad (2g)$$

$d(t)$ [mg/min] is the meal intake. k_m [min] is the inverse of the meal absorption time constant and V_G [dL^{-1}] is the glucose distribution volume.

2.4 CGM Model

We use here the CGM model from Facchinetti et al. (2014). This model represents the glucose transport from plasma to interstitial tissues and the sensor noise. The equation describing glucose transport is

$$dG_I = \frac{1}{\tau_{G,I}} \left(G(t) - G_I(t) \right) dt + \sigma_7 d\omega_7, \quad (2h)$$

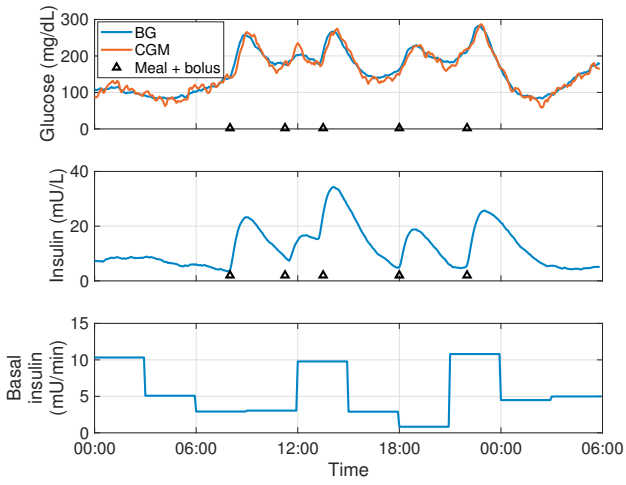

Fig. 3. Example of dataset used for identification.

where the time constant $\tau_{G,I}$ is 6.7 min. The sensor noise is represented by the sum of the two following autoregressive processes

$$cc_k = 1.23cc_{k-1} - 0.3995cc_{k-2} + w_{cc,k}, \tag{3a}$$
$$\hat{v}_k = 1.013\hat{v}_{k-1} - 0.2135\hat{v}_{k-2} + w_k, \tag{3b}$$

in which $w_{cc,k} \sim N(0,11.3\ \text{mg}^2/\text{dL}^2)$ and $w_k \sim N(0,14.45\ \text{mg}^2/\text{dL}^2)$. Thus, the discrete noise-corrupted value returned by the glucose sensor and used in (1b) at the time t_k is

$$y_k = G_I(t_k) + cc_k + \hat{v}_k. \tag{4}$$

2.5 Model identification

The terms related to time constants, k_1, k_2 and p_2, as well as the glucose effectiveness at zero insulin, $GEZI$, are highly uncertain. Therefore, based on our previous work and these observations in Boiroux et al. (2016), we suggest the following simplifications: (i) We use only one term to describe the inverse of the time constants, k_1, k_2 and p_2, (ii) we fix the insulin clearance rate, C_I, because it cannot be distinguished from the insulin sensitivity when only CGM measurements are available, (iii) we set $GEZI = 0$ and (iv) we only identify the diffusion term related to blood glucose concentration, σ_4.

We identify the model parameters in our model using maximum likelihood combined with the continuous-discrete extended Kalman filter described in the next section (Kristensen et al. (2004)). The full details regarding the model identification are provided in Boiroux et al. (2018). Table 1 provides a summary of the identified model parameters for the 10 virtual patients. Fig. 3 shows the BG concentration and CGM measurements, the insulin concentration and the sc. insulin concentration for Patient 1.

3. CONTINUOUS-DISCRETE EXTENDED KALMAN FILTER

The CDEKF is used for state estimation of continuous-discrete grey-box models (Jazwinski (1970); Nørgaard et al. (2000)). In this paper, we use the CDEKF for model identification and in the control algorithm. The filtering in the CDEKF describes the steps used to compute the filtered state, $\hat{x}_{k|k}$, and the corresponding covariance, $P_{k|k}$. The filter step assumes availability of the one-step predictions, $\hat{x}_{k|k-1}$ and $P_{k|k-1}$.

The predictive filter gain is computed by

$$R_{e,k} = C_k P_{k|k-1} C_k' + R, \tag{5a}$$
$$K_k = P_{k|k-1} C_k' R_{e,k}^{-1}, \tag{5b}$$

and the innovation is obtained by

$$e_k = y_k - C_k \hat{x}_{k|k-1}, \tag{6}$$

where

$$C_k = \frac{\partial g}{\partial x}(\hat{x}_{k|k-1}) \tag{7}$$

provides a linearization of the output function g evaluated at $\hat{x}_{k|k-1}$.

The filtered state, $\hat{x}_{k|k}$, and its covariance $P_{k|k}$ are given by

$$\hat{x}_{k|k} = \hat{x}_{k|k-1} + K_k e_k \tag{8a}$$
$$P_{k|k} = P_{k|k-1} - K_k R_{e,k} K_k'. \tag{8b}$$

The predicted mean-covariance pair of the state estimate, $\hat{x}_{k+1|k} = \hat{x}_k(t_{k+1})$ and $P_{k+1|k} = P_k(t_{k+1})$, is computed as the solution to the system of coupled ordinary differential equations (Jørgensen and Jørgensen (2007))

$$\frac{d\hat{x}_k(t)}{dt} = f(t, \hat{x}_k(t), u_k), \tag{9a}$$
$$\frac{dP_k(t)}{dt} = A_k(t)P_k(t) + P_k(t)A_k(t)' + \sigma\sigma', \tag{9b}$$

with

$$A_k(t) = A(t, \hat{x}_k(t), u_k) = \frac{\partial f}{\partial x}(t, \hat{x}_k(t), u_k). \tag{10}$$

The initial conditions for (9a)-(9b) are

$$\hat{x}_k(t_k) = \hat{x}_{k|k}, \tag{11a}$$
$$P_k(t_k) = P_{k|k}. \tag{11b}$$

4. OPTIMAL CONTROL PROBLEM

We assume a zero-order hold parametrization of the input vector, $u(t)$ and the disturbance vector, $d(t)$. At each iteration, the NMPC algorithm will have to solve an optimal control problem in the form

$$\min_{\{x_{k+1},u_k\}_{k=0}^{N-1}} \quad \phi = \sum_{k=0}^{N-1} G_k(x_k, u_k, d_k) + h(x_N) \tag{12a}$$
$$\text{s.t.} \quad b_k := F_k(x_k, u_k, d_k) - x_{k+1} = 0, \tag{12b}$$
$$x(t_0) = x_0, \tag{12c}$$
$$u_{\min} \leq u_k \leq u_{\max}. \tag{12d}$$

The function describing the state dynamics is

$$F_k(x_k, u_k, d_k) = \{x(t_{k+1}) : \dot{x}(t) = f(x(t), u_k, d_k), \\ x(t_k) = x_k\}. \tag{13}$$

The discrete time stage cost is

$$G_k(x_k, u_k, d_k) = \{\int_{t_k}^{t_{k+1}} g(x(t), u_k)dt : \\ \dot{x}(t) = f(x(t), u_k, d_k),\ x(t_k) = x_k\}. \tag{14}$$

In this paper, we use a multiple-shooting based sequential quadratic programming (SQP) algorithm (Bock and Plitt (1984); Diehl et al. (2009); Boiroux et al. (2010a)). The SQP algorithm is used for the numerical solution of (12). We use an explicit Runge-Kutta scheme with fixed stepsize

Table 1. Numerical value of the estimated parameters for the 10 patients.

Patient	k_1, k_2, p_2 (min^{-1})	S_I (mL/mU/min)	EGP_0 (mg/dL/min)	$1/V_G$ (dL^{-1})	k_m (min^{-1})	σ_4 (mg/dL/min)	k_1/k_m (-)
1	0.023	0.0017	1.17	0.0082	0.0226	2.91	1.02
2	0.015	0.0011	0.98	0.004	0.022	3.15	0.68
3	0.021	0.0014	0.87	0.007	0.026	3.15	0.81
4	0.018	0.0019	1.47	0.0059	0.018	3.07	1.00
5	0.012	0.0024	1.57	0.021	0.015	3.28	0.80
6	0.012	0.0018	1.49	0.0020	0.014	3.60	0.86
7	0.014	0.0016	1.07	0.013	0.017	3.13	0.82
8	0.016	0.0011	0.94	0.0036	0.040	3.08	0.44
9	0.014	0.0005	0.35	0.0044	0.041	2.78	0.34
10	0.017	0.0008	0.67	0.0039	0.034	3.14	0.50
Mean	0.017	0.0013	0.958	0.0074	0.027	3.05	0.63

for the numerical integration of the state dynamics, the objective function and for computation of the sensitivities of the objective function and the constraints. The initial state, x_0, is estimated by the CDEKF.

4.1 SQP algorithm

We define the parameter vector, p, as

$$p = \begin{bmatrix} u_0' & x_1' & u_1' & x_2' & \dots & x_{N-1}' & u_{N-1}' & x_N' \end{bmatrix}'. \tag{15}$$

We compute the residuals as

$$b(p) = b(p, x_0, d) = \begin{bmatrix} F_0(x_0, u_0, d_0) - x_1 \\ F_1(x_1, u_1, d_1) - x_2 \\ \vdots \\ F_{N-1}(x_{N-1}, u_{N-1}, d_{N-1}) - x_N \end{bmatrix}. \tag{16}$$

Using these notations, we reformulate the discrete-time OCP (12) as a constrained optimization problem in the standard SQP form

$$\min_p \quad \phi = \phi(p) = \sum_{k=0}^{N-1} G_k(x_k, u_k, d) + h(x_N), \tag{17a}$$

$$\text{s.t.} \quad b(p) = 0, \tag{17b}$$

$$c(p) \geq 0, \tag{17c}$$

in which $c(p)$ corresponds to the bound constraints

$$u_{min} \leq u_k \leq u_{max}. \tag{18}$$

5. OBJECTIVE FUNCTION

In this section, we present and discuss the choice of the objective function. The objective function, ϕ, is a function of the BG concentration, $z(t)$, and the variations in insulin infusion rates, Δu_k. It is

$$\phi = \overbrace{\int_{t_0}^{t_f} \rho_z(z(t))dt}^{\text{BG penalty function}} + \overbrace{\rho_{\Delta u}(\Delta u_k)}^{\text{Insulin penalty term}}. \tag{19}$$

The BG penalty function penalizes the deviation of the predicted BG concentration, $z(t)$, to a given setpoint, $\bar{z}$.

The quadratic glucose penalty function are defined as

$$\rho_{\bar{z}}(z) = \frac{1}{2}(z - \bar{z})^2, \tag{20a}$$

$$\rho_{z_{\min}}(z) = \frac{1}{2}\left(\min\{z - z_{\min}, 0\}\right)^2, \tag{20b}$$

$$\rho_{z_{\max}}(z) = \frac{1}{2}\left(\max\{z - z_{\max}, 0\}\right)^2, \tag{20c}$$

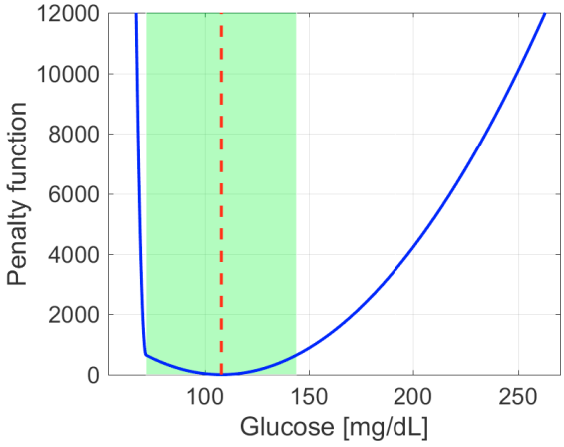

Fig. 4. The asymmetric penalty function.

where $\bar{z}$ is the desired glucose target. $z_{\min}$ and $z_{\max}$ are thresholds for hypoglycemia (BG<70 mg/dL) and hyperglycemia (BG>180 mg/dL), respectively. The resulting penalty function is

$$\rho_z(z) = \alpha_{\bar{z}}\rho_{\bar{z}}(z) + \alpha_{z_{\min}}\rho_{z_{\min}}(z) + \alpha_{z_{\max}}\rho_{z_{\max}}(z), \tag{21}$$

in which $\alpha_{\bar{z}}$, $\alpha_{z_{\min}}$ and $\alpha_{z_{\max}}$ are weights. Since hypoglycemia is much more undesirable than hyperglycemia and postprandial hyperglycemia is unavoidable, we set high penalties for BG concentrations below 4 mmol/L and we do not set any additional penalty on hyperglycemic BG concentrations, ie. $\alpha_{z_{\max}} = 0$. Fig. 4 illustrates the asymmetrical cost function.

It is possible to normalize the weight on the ℓ_2 penalty for Δu by setting the following scaling

$$\rho_{\Delta u}(\Delta u) = \frac{1}{2}\frac{\alpha_{\Delta u}}{T_s}\Delta u^2, \tag{22a}$$

in which T_s is the sampling time, such that the tuning of the controller remains identical regardless of the sampling time.

6. RESULTS

In this section, we evaluate the closed-loop performance of our NMPC-based control algorithm using numerical simulations of a stochastic model. To simulate the intra-patient variability, we consider a SDE version of the T1D model in the form of (1). The model for simulation is derived from the model and the parameter distribution developed by (Hovorka et al., 2002). We use the Euler-Maruyama

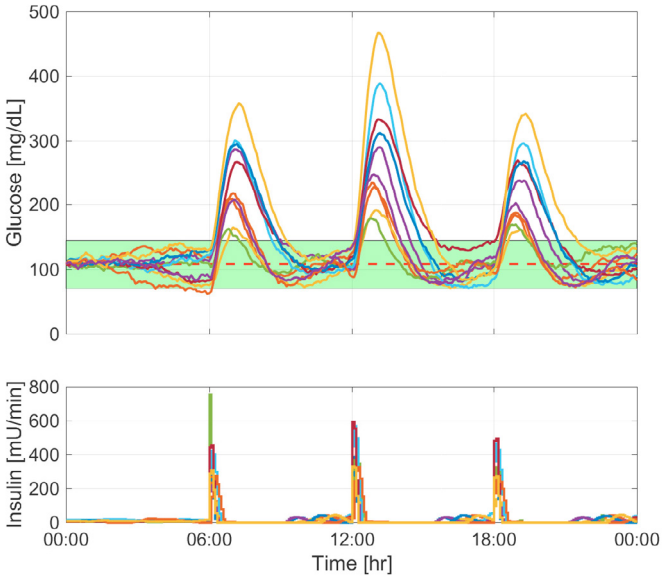

(a) BG concentration profile (top) and sc. insulin administration profile (bottom).

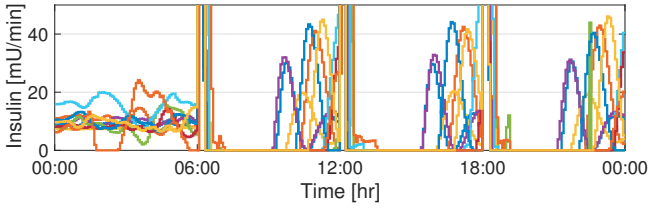

(b) Zoom on the insulin administration profile.

Fig. 5. BG concentration and insulin traces for the 10 virtual patients.

method for numerical integration, see eg. Higham (2001). The patients have the following meals: a 75g CHO breakfast at 6:00, a 100g CHO lunch at 12:00 and a 75g CHO dinner at 18:00. The meals are announced to the controller at mealtimes only. We set $u_{\min} = 0$ to allow insulin suspension and we set the maximal insulin infusion rate, $u_{\max}$, to a large value such that it is not limiting the performance of the control algorithm.

Fig. 5 shows the BG concentration traces and the insulin infusion rates for the 10 virtual patients. The variability between the patients becomes large after meals, depending on the sc. insulin and meal absorption time constants. The insulin profile shows a bolus-like impulse followed by a suspension of insulin delivery for all patients, sometimes referred to as a super-bolus. Clinical studies have shown that using a super-bolus strategy tightens the regulation of BG concentration and reduces the occurrence of postprandial hypoglycemia (Rossetti et al. (2012); Boronat et al. (2015)).

Fig. 6 depicts the control variability grid analysis (CVGA) plot for the 10 patients. Only one patient had a mild hypoglycemic event before breakfast. The large postprandial glucose excursions are mainly caused by the large meal sizes and the ratio between time-to-peak of meal absorption and time-to-peak of insulin absorption (Boiroux et al. (2010b); El Fathi et al. (2018)).

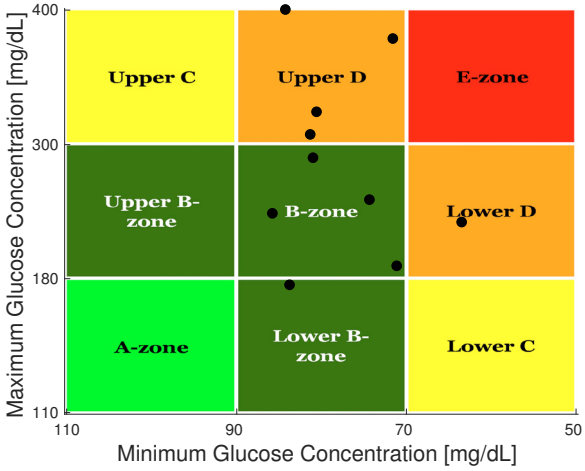

Fig. 6. Control variability grid analysis (CVGA) for the 10 virtual patients (Magni et al. (2008)).

Table 2. Percentage of time spent in different BG concentration ranges. The numbers show the median and the interquartile range (IQR).

	Median	IQR
$BG > 180$ mg/dL (%)	16.6	9.0-25.3
$70 \leq BG \leq 180$ mg/dL (%)	82.2	74.7-91.0
$70 \leq BG \leq 140$ mg/dL (%)	73.0	61.8-81.3
$BG < 70$ mg/dL (%)	0	0-0

The simulation results provide insight into the ideal insulin delivery profile and the maximum achievable performance of an AP system. For patients with elevated postprandial peaks, safety considerations would preclude from administering large amounts of insulin ahead of meals. Instead, an adapted diet consisting of lower CHO amounts and slower sugars could reduce postprandial glucose excursions.

Table 2 shows the BG concentration median percentage of time spent in target, hypo- and hyperglycemia. The table shows the median and interquartile range. We see that most of the time is spent in euglycemic range. However, the time spent in hyperglycemia varies and highly depends on the meal and insulin absorption dynamics.

7. CONCLUSION

In this paper we developed an NMPC-based control algorithm. Parameter identification is used to handle inter-patient variability and to adjust for long-term metabolic variations. We numerically evaluated the performance of our control algorithm. The results suggest that the estimation of model parameters involved in NMPC algorithms using CGM data is promising for the design of an AP. Currently, the slow insulin dynamics compared to CHO absorption dynamics limit the performance of the AP. Personalized diet in complement to control algorithms could further improve glucose regulation by reducing postprandial peaks.

REFERENCES

Bock, H. and Plitt, K. (1984). A multiple shooting method for direct solution of optimal control problems. In *Proc.*

of the IFAC 9th World Congress, 242–247. Budapest, Hungary.

Boiroux, D., Aradóttir, T., Hagdrup, M., Poulsen, N., Madsen, H., and Jørgensen, J.B. (2015). A bolus calculator based on continuous-discrete unscented Kalman filtering for type 1 diabetics. In *9th IFAC Symposium on Biological and Medical Systems*, 159 – 164.

Boiroux, D., Finan, D.A., Poulsen, N.K., Madsen, H., and Jørgensen, J.B. (2010a). Nonlinear model predictive control for an artificial β-cell. In *Recent Advances in Optimization and its Applications in Engineering*, 299 – 308. Springer.

Boiroux, D., Finan, D.A., Poulsen, N.K., Madsen, H., and Jørgensen, J.B. (2010b). Optimal insulin administration for people with type 1 diabetes. In *Proceedings of the 9th International Symposium on Dynamics and Control of Process Systems (DYCOPS 2010)*, 234 – 239.

Boiroux, D., Aradóttir, T.B., Nørgaard, K., Poulsen, N.K., Madsen, H., and Jørgensen, J.B. (2017). An adaptive nonlinear basal-bolus calculator for patients with type 1 diabetes. *Journal of Diabetes Science and Technology*, 11(1), 29–36.

Boiroux, D., Hagdrup, M., Mahmoudi, Z., Poulsen, N.K., Madsen, H., and Jørgensen, J.B. (2016). Model identification using continuous glucose monitoring data for type 1 diabetes. *IFAC-PapersOnLine*, 49(7), 759–764.

Boiroux, D., Mahmoudi, Z., and Jørgensen, J.B. (2018). Parameter estimation in type 1 diabetes models for model-based control applications. In *2018 IEEE Conference on Control Technology and Applications (CCTA2018)*. Submitted.

Boronat, M., Sánchez-Hernández, R.M., Rodríguez-Cordero, J., Jiménez-Ortega, A., and Nóvoa, F.J. (2015). Suspension of basal insulin to avoid hypoglycemia in type 1 diabetes treated with insulin pump. *Endocrinology, Diabetes & Metabolism Case Reports*, 2015.

Diehl, M., Ferreau, J., and Haverbeke, N. (2009). Efficient numerical methods for nonlinear MPC and moving horizon estimation. In *Nonlinear Model Predictive Control. Towards New Challenging Applications*, 391–417. Springer, Berlin, Germany.

El Fathi, A., Smaoui, M.R., Gingras, V., Boulet, B., and Haidar, A. (2018). The artificial pancreas and meal control: An overview of postprandial glucose regulation in type 1 diabetes. *IEEE Control Systems Magazine*, 38(1), 67–85.

Facchinetti, A., Del Favero, S., Sparacino, G., Castle, J.R., Ward, W.K., and Cobelli, C. (2014). Modeling the glucose sensor error. *IEEE Transactions on Biomedical Engineering*, 61(3), 620–629.

Higham, D.J. (2001). An algorithmic introduction to numerical simulation of stochastic differential equations. *SIAM Review*, 43(3), 525–546.

Hovorka, R., Canonico, V., Chassin, L.J., Haueter, U., Massi-Benedetti, M., Federici, M.O., Pieber, T.R., Schaller, H.C., Schaupp, L., Vering, T., and Wilinska, M.E. (2004). Nonlinear model predictive control of glucose concentration in subjects with type 1 diabetes. *Physiological Measurement*, 25, 905–920.

Hovorka, R., Shojaee-Moradie, F., Caroll, P.V., Chassin, L.J., Gowrie, I.J., Jackson, N.C., Tudor, R.S., Umpleby, A.M., and Jones, R.H. (2002). Partitioning glucose distribution/transport, disposal, and endogenous production during IVGTT. *American Journal of Physiology*, 282, 992–1007.

Jazwinski, A.H. (1970). *Stochastic Processes and Filtering Theory*. Academic Press, San Diego, CA.

Jørgensen, J.B. and Jørgensen, S.B. (2007). Comparison of prediction-error modelling criteria. In *Proceedings of the 2007 American Control Conference (ACC 2007)*, 140–146.

Kanderian, S.S., Weinzimer, S., Voskanyan, G., and Steil, G.M. (2009). Identification of intraday metabolic profiles during closed-loop glucose control in individuals with type 1 diabetes. *Journal of Diabetes Science and Technology*, 3(5), 1047 – 1057.

Kristensen, N.R., Madsen, H., and Jørgensen, S.B. (2004). Parameter estimation in stochastic grey-box models. *Automatica*, 40, 225 – 237.

Magni, L., Raimondo, D., Man, C.D., Breton, M., Patek, S., Nicolao, G.D., Cobelli, C., and Kovatchev, B. (2008). Evaluating the efficacy of closed-loop glucose regulation via control-variability grid analysis. *Journal of Diabetes Science and Technology*, 2(4), 630 – 635.

Mahmoudi, Z., Boiroux, D., Hagdrup, M., Kj, N., Madsen, H., Bagterp, J., et al. (2016). Application of the continuous-discrete extended Kalman filter for fault detection in continuous glucose monitors for type 1 diabetes. In *2016 European Control Conference (ECC 2016)*, 714–719.

Mahmoudi, Z., Nørgaard, K., Poulsen, N.K., Madsen, H., and Jørgensen, J.B. (2017). Fault and meal detection by redundant continuous glucose monitors and the unscented Kalman filter. *Biomedical Signal Processing and Control*, 38, 86–99.

Marchetti, G., Barolo, M., Jovanovič, L., Zisser, H., and Seborg, D.E. (2008). A feedforward-feedback glucose control strategy for type 1 diabetes mellitus. *Journal of Process Control*, 18(2), 149–162.

Nørgaard, M., Poulsen, N.K., and Ravn, O. (2000). New developments in state estimation for nonlinear systems. *Automatica*, 36, 1627–1638.

Rossetti, P., Ampudia-Blasco, F.J., Laguna, A., Revert, A., Vehì, J., Ascaso, J.F., and Bondia, J. (2012). Evaluation of a novel continuous glucose monitoring-based method for mealtime insulin dosingthe ibolusin subjects with type 1 diabetes using continuous subcutaneous insulin infusion therapy: a randomized controlled trial. *Diabetes Technology & Therapeutics*, 14(11), 1043–1052.

Samadi, S., Rashid, M., Turksoy, K., Feng, J., Hajizadeh, I., Hobbs, N., Lazaro, C., Sevil, M., Littlejohn, E., and Cinar, A. (2018). Automatic detection and estimation of unannounced meals for multivariable artificial pancreas system. *Diabetes Technology & Therapeutics*, 20(3), DOI: 10.1089/dia.2017.0364.

Schmidt, S., Meldgaard, M., Serifovski, N., Storm, C., Christensen, T.M., Gade-Rasmussen, B., and Nørgaard, K. (2012). Use of an automated bolus calculator in MDI-treated type 1 diabetes. *Diabetes Care*, 35(5), 984–990.

Turksoy, K., Samadi, S., Feng, J., Littlejohn, E., Quinn, L., and Cinar, A. (2016). Meal detection in patients with type 1 diabetes: a new module for the multivariable adaptive artificial pancreas control system. *IEEE Journal of Biomedical and Health Informatics*, 20(1), 47–54.